



Effect of Precipitation Time on Structure and Properties of Li-Rich Cathode Materials ($\text{Li}_{1.2}\text{Ni}_{0.15}\text{Co}_{0.10}\text{Mn}_{0.55}\text{O}_2$) Prepared by Co-deposition Method

Ruiming Yang^{a,b}, Yingjie Zhang^{a,*}, Peng Dong^a, Yannan Zhang^a

^aNational and Local Joint Engineering Laboratory for Lithium-ion Batteries and Materials Preparation Technology, Key Laboratory of Advanced Battery Materials of Yunnan Province, Faculty of Materials Science and Engineering, Kunming University of Science and Technology, Kunming 650093, China

^bCollege of Physics and Electronic Engineering, Qujing Normal University, Qujing 655011, China
 zyjkmust@126.com

The lithium Li-rich cathode material $\text{Li}_{1.2}\text{Ni}_{0.15}\text{Co}_{0.10}\text{Mn}_{0.55}\text{O}_2$ was prepared by one combined method of coprecipitation and solid phase sintering. The morphology, phase and electrochemical properties of the samples at different precipitation times were tested by SEM, XRD, battery test system and electrochemical workstation. The results show that the morphology and electrochemical properties of the prepared cathode materials can be effectively controlled by controlling the precipitation time during the coprecipitation process. At the precipitation time of 8h, the precursor prepared has regular morphology and the best dispersibility. Under the voltage range of 2.0–4.8V and 0.1C, the retention rate at 50-cycle capacity is 80.0%, and the discharge specific capacity at 5C can reach $131 \text{ mAh}\cdot\text{g}^{-1}$; at the same time, the sample prepared at this precipitation time has a lower electrochemical transfer resistance of 159Ω . Through this study, it is verified that the control of the precipitation time in the coprecipitation process can effectively regulate the structure of the cathode material and improve its electrochemical performance.

1. Introduction

In recent years, thanks to their high specific capacity, li-rich manganese based cathode materials $x\text{Li}_2\text{MnO}_3(1-x)\text{LiMO}_2(\text{M}=\text{Ni, Co, Mn, etc.})$ have attracted much attention, and become one of the ideal cathode materials. Different preparation methods, synthesis processes, selected raw materials, etc. all have a great influence on the morphology and properties of li-rich cathode materials (Kong et al., 2015).

The coprecipitation method + high temperature solid phase sintering method has great advantages in synthesizing materials and controlling production costs (Chi et al., 2018; Jin et al., 2016). At present, most scholars pay attention to the influence of sintering time and sintering process on morphology and performance. However, in the preparation process of coprecipitation, the precipitation time shall affect the size and shape of the sample, and further influence the material properties, which has been rarely discussed in related studies.

Based on this, the li-rich cathode material $\text{Li}_{1.2}\text{Ni}_{0.15}\text{Co}_{0.10}\text{Mn}_{0.55}\text{O}_2$ was synthesized by the combination of coprecipitation method and high temperature solid phase sintering method in this paper, and the effects of precipitation time on the morphology and phase of the precursor were studied by SEM and XRD. Then, Electrochemical testing was conducted to mainly study the effect of precipitation time on the charge-discharge property and cycle life of the precursor. This study shall provide guidance for the preparation of high performance li-rich cathode materials by coprecipitation + high temperature solid phase sintering (Zhao et al., 2013; Zheng et al., 2014).

2. Experiments

2.1 Material preparation

2.1.1 Preparation of precursors

Firstly, 1000ml of solution with a total metal cation concentration of 2 mol/L, and a sulfate solution of Ni, Co, and Mn were prepared at a molar ratio of Ni-Co-Mn 0.1625:0.1625:0.675. Then, 1000ml Na_2CO_3 solution at 2 mol/L and 1000ml ammonia water at 1 mol/L were separately prepared. The reaction was carried out in a “coprecipitation reactor”, and the solution was added to the glass double-layer reactor at a rotation speed of 500r/min according to the reaction stoichiometric ratio, while adding a certain amount of ammonia water, by strictly controlling the flow rate of the solution, and the reaction pH value at about 8.2. When the transition metal salt solution was completely added to the precipitant solution, it's recorded as the time zero. After making reaction at 50 °C for 2 h, 4 h, 6 h, 8 h, 10 h and 12 h (respectively referred to as S-2, S-4, S-6, S-8, S-10 and S-12), it's washed with hot deionized water for 5 to 7 times until the pH of the solution is close to neutral. Finally, it was dried at 80 °C for 12h to obtain a carbonate precursor of the mixed metal of Ni, Co, and Mn.

2.1.2 Lithium sintering

The precursor of $\text{Ni}_{0.1675}\text{Co}_{0.1625}\text{Mn}_{0.675}\text{CO}_3$ and lithium hydroxide (LiOH) were mixed. The molar ratio of Li to the total metal cations in carbonate was 1.5:1, and the excess of Li source was 5%. Lithium hydroxide was added and milled at 500 rpm for 2h. Then, it was placed in a box-type resistance furnace, heated to 850°C at the temperature rise of 20° C/min in an air atmosphere, and kept for 12h. Finally, it's cooled to room temperature with a furnace to obtain a li-rich cathode material $\text{Li}_{1.2}\text{Ni}_{0.15}\text{Co}_{0.10}\text{Mn}_{0.55}\text{O}_2$.

2.2 Micromorphology and phase characterization

The 1530Vp scanning electron microscope by Germany LEO was adopted to characterize the surface morphology of the sample (acceleration potential 5 kV). The morphology of the sample was observed using a Tecnai G2 20 S-TWIN type transmission electron microscope of German FEI company. The phase composition of the sample was analysed using a D8 ADVANCE automatic X-ray diffractometer by German Drucker: X-ray source is Cu K α (1486.6 eV, $\lambda = 0.15406$ nm), the operating potential is 30 kV, the current is 30 kV and 30 mA, the step length is 0.5°, and the diffraction angle is $10^\circ \leq 2\theta \leq 80^\circ$.

2.3 Battery assembly and electrochemical property test

The prepared positive electrode materials $\text{Li}_{1.2}\text{Ni}_{0.15}\text{Co}_{0.1}\text{Mn}_{0.55}\text{O}_2$, PVDF, Ks-6, and super P were mixed in an appropriate amount of NMP at a ratio of 24:3:2:1. The mixture was stirred at room temperature for 3 hours to obtain a well-proportional pasty mass, which was uniformly coated on an aluminium foil and vacuum-dried in a drying oven at 120°C for 12 hours. After rolling on the roller press under a pressure of about 12MP, the rolled material was placed on a battery slicer to obtain the desired electrode slice with a diameter of 14 mm. The negative electrode is made of lithium metal plate, the Celgard 2400 porous polyethylene film is used as the membrane, and the electrolyte is LiPF6 at 1mol/L; the solvent is ethylene carbonate (EC), dimethyl carbonate (DMC), methyl ethyl carbonate (EMC), with a volume ratio of 1:1:1. Finally, the CR2025 button battery was assembled (Yu et al., 2014; Zheng et al., 2018).

The battery was subjected to constant current charge and discharge test using the current test system of Wuhan Landian Electronics Co., Ltd, and the charge and discharge voltage range was 2-4.8V. The electrochemical impedance spectroscopy of the material was tested by the PGSTAT302N electrochemical workstation manufactured by Switzerland Metrohm, with the scanning rate of 0.2 mV s $^{-1}$, the voltage range of 2-4.8 V, and the electrochemical tests were performed at room temperature of 25 °C.

3. Results and discussions

3.1 Micromorphology and phase

Figure 1 (a-f) show the morphology of Ni-Co-Mn precursor prepared by coprecipitation at different precipitation times. As the precipitation time prolonged during the preparation of the precursor, the particles became larger, and the irregular particles gradually crystallized to form a uniform sphere. However, as the precipitation time was further extended, the spherical particles gradually agglomerated and the dispersibility deteriorated. Figure 1(a) and (b) show that when the precipitation time is less than 4h, the prepared precursor has an irregular morphology, which is a mixture of small particles and spheres; Figure 1(c), (d), and (e) indicate that when the precipitation time is 6 to 10h, the prepared precursor is substantially spherical and has a relatively regular shape. At 8h, the spherical particles have better dispersibility and are more uniform; Figure 1(f) shows very

serious precursor agglomeration and poor dispersibility when the precipitation time reaches 12h. Through the analysis of the precursor micromorphology, when the Ni-Co-Mn precursor is prepared by the co-precipitation method, the particles formed are the most regular and the dispersion is the best at the precipitation time of 8h.

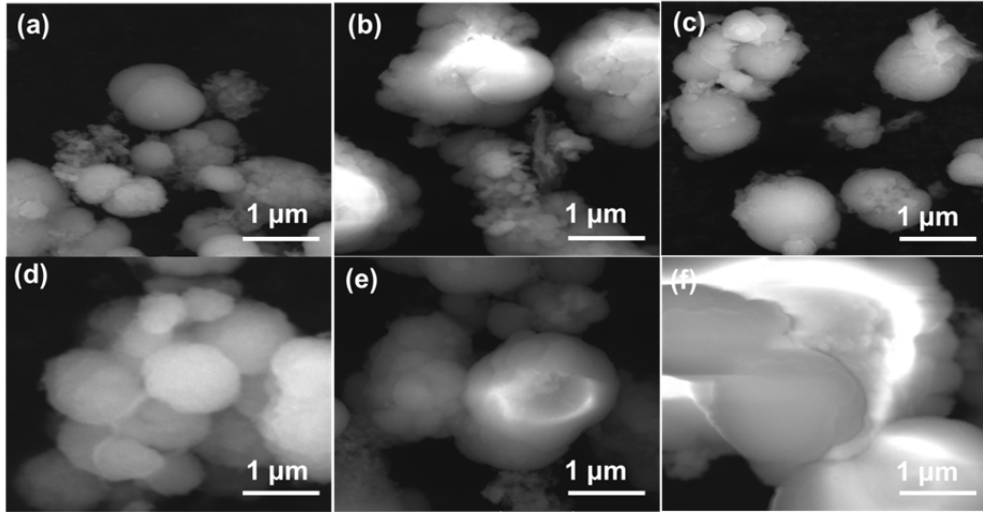


Figure 1: SEMs of precursors prepared by coprecipitation at different precipitation times (a) 2 h (b) 4 h (c) 6 h (d) 8 h (e) 10 h (f) 12 h

Figure 2(a) shows that there is no impurity phase in the Ni-Co-Mn precursor prepared without precipitation, and its structure is the same as that of MnCO₃ (PDF#44-1472), which is a trigonal crystal system in the calcite crystal form.

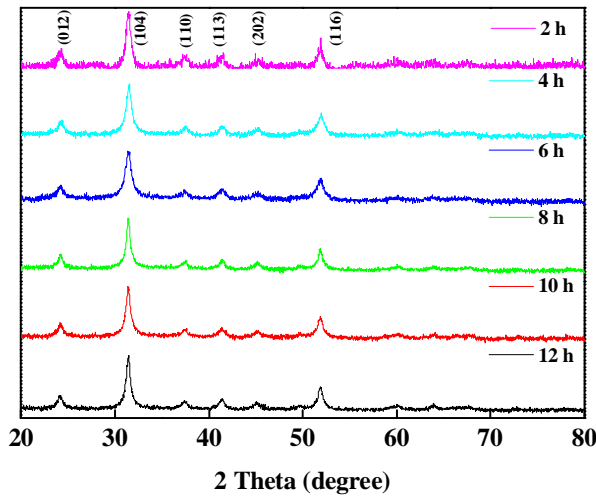


Figure 2: Precursor XRD prepared by coprecipitation at different precipitation times (a) 2h (b) 4h (c) 6h (d) 8h (e) 10h (f) 12h

Through SEM and XRD analysis, it can be seen that the precursor prepared at the precipitation time of 6-10h was basically spherical, but having the most uniform morphology at 8h. In order to further analyse the effect of precipitation time on properties, the precursors prepared under the conditions of precipitation time of 6h, 8h and 10h were respectively subjected to high temperature solid phase sintering, and the electrochemical properties of the prepared materials were characterized (Lee et al., 2015; Lim et al., 2015; Szklarz et al., 2016; Yang et al., 2018).

3.2 Electrochemical property

Figure 3 shows the curve of specific discharge capacity cycling at 0.1C current density (1C=200 mA g⁻¹) for samples prepared at different precipitation times. It can be seen from the figure that the initial discharge specific capacity of the samples prepared at the precipitation time of 6h, 8h and 10h were 215mAh g⁻¹, 227

mAh g^{-1} , 226 mAh g^{-1} , respectively, and at the precipitation time of 8h, the sample prepared under the conditions had the highest specific discharge capacity at the first time. After 50 cycles of charge and discharge at 0.1C, the capacities of samples S-6, S-8 and S-10 were 171 mAh g^{-1} , 177 mAh g^{-1} , 172 mAh g^{-1} , respectively. After 50 cycles, the capacity retention rates were 79.5%, 80.0%, and 76.1%, respectively. In summary, the sample prepared at the precipitation time of 8h has the highest specific discharge capacity and cycle stability, which is mainly due to the uniform distribution of these sample particles (Wu et al., 2015).

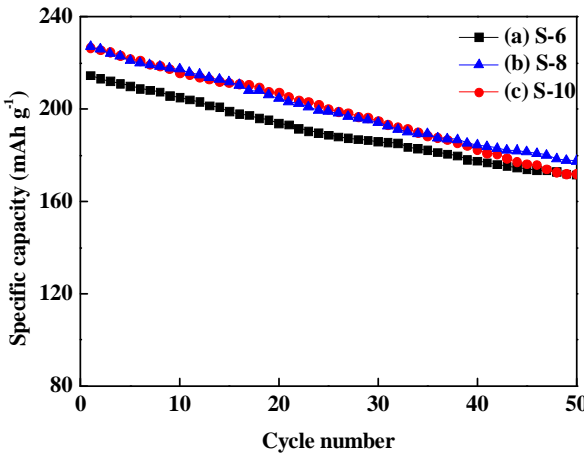


Figure 3: Cyclic performance of samples prepared at different precipitation times at 2-4.8 V, and 0.1 C (a) 6h (b) 8h (c) 10h

Figure 4 shows the rate performance of samples prepared at different precipitation times. At 0.1C, 1C, 2C rate, the discharge specific capacities of S-8 and S-10 were close, and both were higher than S-6, but with the further increase of the discharge rate, the specific discharge capacity of S-8 was much higher than that of S-6 and S-10; at the large rate of 5C, the specific discharge capacity of S-8 was 131 mAh g^{-1} , which was 10 mAh g^{-1} and 5 mAh g^{-1} higher than S-6 and S-8 respectively, indicating that the sample prepared at the precipitation time of 8h has the best rate performance. This is mainly because the uniform morphology is more favourable for the positive electrode material to maintain the structural stability under the impact of large rate current (Liu et al., 2013; Yan et al., 2014).

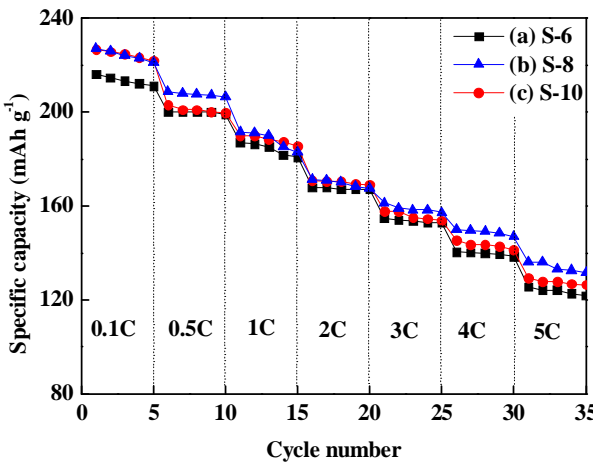


Figure 4: Rate performance of samples prepared at different precipitation times (a) 6h (b) 8h (c) 10h

The fitting results of electrochemical impedance spectroscopy by Zview are shown in Figure 5. The specific values are shown in Table 1. R_s characterizes the solution resistance of the reference electrode to the working electrode, and R_{ct} characterizes the charge transfer resistance of the electrode. It can be seen from Table 1 that the R_s and R_{ct} of the samples prepared under the precipitation time of 8 h are less than those at 10 h and 6 h, indicating that the sample prepared under the 8h has a smaller interface impedance and charge transfer impedance (Lin et al., 2015; Mohanty et al., 2013; Lu et al., 2018).

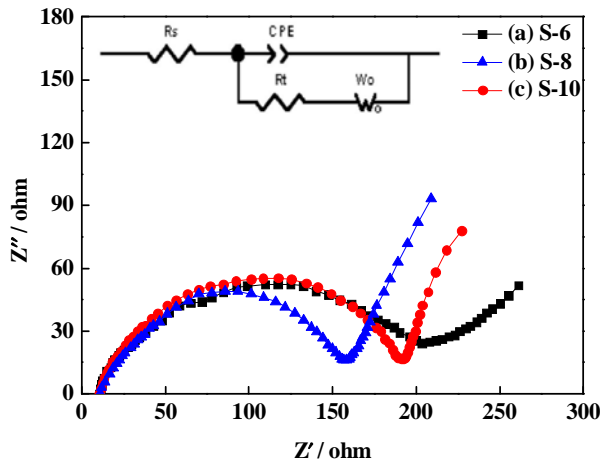


Figure 5: Electrochemical impedance spectroscopy of samples prepared at different precipitation times (a) 6h (b) 8h (c) 10h

Table 1: Rs and Rct values of different samples by equivalent circuit fitting

Sample	Rs/ohm	Rct/ohm
S-6	10.9	203.4
S-8	10.4	156.9
S-10	10.7	191.1

4. Conclusions

In the process of preparing the precursor $\text{Ni}_{0.1675}\text{Co}_{0.1625}\text{Mn}_{0.675}\text{CO}_3$ by co-precipitation method, the precipitation time directly affects the morphology of the precursor, further influencing the electrochemical properties of the material. With the prolongation of precipitation time, the particle size of the precursor material gradually increases; under the condition of 8h precipitation time, the precursor particles prepared are the most uniform and the dispersity is the best. The lithium-rich cathode material $\text{Li}_{1.2}\text{Ni}_{0.15}\text{Co}_{0.10}\text{Mn}_{0.55}\text{O}_2$ synthesized by the precursor prepared under this condition after high-temperature solid phase sintering with lithium has higher discharge specific capacity, cycle stability, rate performance and smaller charge transfer impedance. Therefore, the structure and electrochemical properties of the lithium-rich cathode material $\text{Li}_{1.2}\text{Ni}_{0.15}\text{Co}_{0.10}\text{Mn}_{0.55}\text{O}_2$ can be effectively improved by the control of the precipitation time. This also may provide new ideas for the preparation of other high-performance lithium-rich cathode materials.

References

- Chi M.S., Wang Q., Liu H.Q., Wang Z.C., Liu Q., 2018, Characteristic analysis of gas & solid phase flow in oil shale pyrolysis circulating fluidized bed, International Journal of Heat and Technology, 36(1), 159-164, DOI: 10.18280/ijht.360121
- Jin X., Xu Q., Liu X., Yuan X.L., Liu H.M., 2016, Improvement in rate capability of lithium-rich cathode material $\text{Li}[\text{Li}_{0.2}\text{Ni}_{0.13}\text{Co}_{0.13}\text{Mn}_{0.54}\text{O}_2]$ by Mo substitution, Ionics, 22(8), 1369-1376, DOI: 10.1007/s11581-016-1675-4
- Kong J.Z., Wang C.L., Qian X., Tai G.A., Li A.D., Wu D., Li H., Zhou F., Yu C., Sun Y., Jia D., Tang W.P., 2015, Enhanced electrochemical performance of $\text{Li}_{1.2}\text{Mn}_{0.54}\text{Ni}_{0.13}\text{Co}_{0.13}\text{O}_2$ by surface modification with graphene-like lithium-active MoS_2 , Electrochimica Acta, 174(20), 542-550, DOI: 10.1016/j.electacta.2015.05.185
- Lee E., Koritala R., Miller D.J., Johnson C.S., 2015, Aluminum and Gallium Substitution into $0.5\text{Li}_2\text{MnO}_3\cdot0.5\text{Li}(\text{Ni}_{0.375}\text{Mn}_{0.375}\text{Co}_{0.25})\text{O}_2$ Layered Composite and the Voltage Fade Effect, Journal of the Electrochemical Society, 162(3), 322-329, DOI: 10.1149/2.0321503jes
- Lim S.N., Seo J.Y., Jung D.S., Park S.B., Yeon S.H., 2015, The crystal structure and electrochemical performance of $\text{Li}_{1.167}\text{Mn}_{0.548}\text{Ni}_{0.18}\text{Co}_{0.105}\text{O}_2$, composite cathodes doped and co-doped with Mg and F[J]. Journal of Electroanalytical Chemistry, 740, 88-94, DOI: 10.1016/j.jelechem.2015.01.010
- Lin M., Ben L., Sun Y., Wang H., Yang Z.Z., Gu L., Yu X.Q., Yang X.Q., Zhao H.F., Yu R.C., Armand M., Huang X.J., 2015, Insight into the Atomic Structure of High-Voltage Spinel $\text{LiNi}_{0.5}\text{Mn}_{1.5}\text{O}_4$ Cathode Material in the First Cycle, Chemistry of Materials, 27(1), 292-303, DOI: 10.1021/cm503972a

- Liu G.B., Liu H., Wang Y., Shi Y.F., Zhang Y., 2013, The electrochemical properties of Fe- and Ni-cosubstituted Li_2MnO_3 , via combustion method, *Journal of Solid State Electrochemistry*, 17(9), 2437-2444, DOI: 10.1007%2Fs10008-013-2127-y
- Lu M., 2018, Effect of rare earth oxide on electrochemical behaviors of ni-mh battery on new energy vehicle, *Chemical Engineering Transactions*, 66, 91-96, DOI:10.3303/CET1866016
- Martha S.K., Sclar H., Szmuk Framowitz Z., 2009, A comparative study of electrodes comprising nanometric and submicron particles of $\text{LiNi}_{0.50}\text{Mn}_{0.50}\text{O}_2$, $\text{LiNi}_{0.33}\text{Mn}_{0.33}\text{Co}_{0.33}\text{O}_2$, and $\text{LiNi}_{0.40}\text{Mn}_{0.40}\text{Co}_{0.20}\text{O}_2$ layered compounds, *Journal of Power Sources*, 189(1), 248-255.
- Mohanty D., Huq A., Payzant E.A., Safat A., Li J., Abraham D., Daniel C., 2013, Neutron Diffraction and Magnetic Susceptibility Studies on a High-Voltage $\text{Li}_{1.2}\text{Mn}_{0.55}\text{Ni}_{0.15}\text{Co}_{0.10}\text{O}_2$ Lithium Ion Battery Cathode: Insight into the Crystal Structure, *Chemistry of Materials*, 25(20), 4064-4070, DOI: 10.1021/cm402278q
- Szklarz Z., Krawiec H., Rogal Ł., 2016, Effect of the cooling rate on the electrochemical behaviour of 2017 aluminium alloy, *Annales de Chimie: Science des Materiaux*, 40(1-2), 25-32, DOI: 10.3166/acsm.40.25-32
- Wu F., Zhang X., Zhao T., Li L., Xie M., Chen R., 2015, Multifunctional AlPO_4 coating for improving electrochemical properties of low-cost $\text{Li}[\text{Li}_{0.2}\text{Fe}_{0.1}\text{Ni}_{0.15}\text{Mn}_{0.55}]\text{O}_2$ cathode materials for lithium-ion batteries, *Acs Appl. Mater. Interfaces*, 7(6), 3773-3781, DOI: 10.1021/am508579r
- Yan J., Liu X., Li B., 2014, Recent progress in Li-rich layered oxides as cathode materials for Li-ion batteries, *Rsc Advances*, 4(108), 63268-63284, DOI: 10.1039/C4RA12454E
- Yang R., Zhang Y., Dong P., 2018, The Effect of Heating Rate on the Structure and Electrochemical Performance of the Li-rich Cathode Material $\text{Li}_{1.2}\text{Ni}_{0.15}\text{Co}_{0.10}\text{Mn}_{0.55}\text{O}_2$ Prepared Using the Co-precipitation Method, *Int. J. Electrochem. Sci*, 13, 8116-8126.
- Yu K., Lyu C., Gu L., Wu H., Bak S., Zhou Y., Amine K., Ehrlich S., Li H., Nam K., Yang X., 2014, Understanding the Rate Capability of High-Energy-Density Li-Rich Layered $\text{Li}_{1.2}\text{Ni}_{0.15}\text{Co}_{0.1}\text{Mn}_{0.55}\text{O}_2$ Cathode Materials, *Advanced Energy Materials*, 4(5), DOI: 10.1002/aenm.201300950
- Zhao C., Liu R., Liu X., Wang X., Feng F., Sheng Q., 2013, Sacrificed template synthesis of $\text{Li}_{1.2}\text{Ni}_{0.13}\text{Co}_{0.13}\text{Mn}_{0.54}\text{O}_2$ spheres for lithium-ion battery cathodes, *Journal of Nanoparticle Research*, 15(11), 2064, DOI: 10.1007%2Fs11051-013-2064-9
- Zheng J., Gu M., Xiao J., Polzin B., Yan P., Chen X., Wang C., Zhang J.G., 2014, Functioning Mechanism of AlF_3 Coating on the Li-and Mn-Rich Cathode Materials, *Chemistry of Materials*, 26(22), 6320-6327, DOI: 10.1021/cm502071h
- Zheng M.G., Zhang Y.K., Shi L., 2018, Research on selective non-catalytic NOx reduction (SNCR) for diesel engine, *International Journal of Heat and Technology*, 36(3), 981-986, DOI: 10.18280/ijht.360326